

Composition determination of β -(Al_xGa_{1-x})₂O₃ layers coherently grown on (010) β -Ga₂O₃ substrates by high-resolution x-ray diffraction

Yuichi Oshima^{1*}, Elaheh Ahmadi¹, Stefan C. Badescu², Feng Wu¹, and James S. Speck¹

¹*University of California, Santa Barbara, CA, 93106 USA*

²*Wright Patterson Air Force Base, Sensors Directorate, Dayton, OH 45433, USA*

E-mail: yuichi@engineering.ucsb.edu

We demonstrate x-ray diffraction based composition estimation of β -(Al_xGa_{1-x})₂O₃ coherently grown on (010) β -Ga₂O₃. The relation between the strain along the [010] direction and the Al composition of the β -(Al_xGa_{1-x})₂O₃ layer was formulated by using stress-strain relationship in the monoclinic system. This formulation allows us to estimate the Al composition using out-of-plane lattice spacing determined by conventional x-ray ω - 2θ measurements. This method was applied to MBE-grown coherent β -(Al_xGa_{1-x})₂O₃/Ga₂O₃ heterostructures, and the Al composition in the β -(Al_xGa_{1-x})₂O₃ are in close agreement with composition determined directly by atom probe tomography.

β -Ga₂O₃ is a wide bandgap semiconductor ($E_g = 4.7 - 4.9$ eV),¹⁻³⁾ which crystalizes in the monoclinic structure. β -Ga₂O₃ is attracting a remarkable attention due to its great potential to realize power devices with higher breakdown voltages and lower energy losses than its counterparts GaN and SiC. In reality, several promising results have already been reported on β -Ga₂O₃ based power devices such as Schottky barrier diodes,⁴⁾ metal-semiconductor field effect transistors (MESFETs),⁵⁾ and metal-oxide field effect transistors (MOSFETs).⁶⁾ In addition, β -(Al_xGa_{1-x})₂O₃ solid solutions and β -(Al_xGa_{1-x})₂O₃/ β -Ga₂O₃ hetero-structures have been studied intensively since these will enable band engineering and lead to the realization of further high-performance β -Ga₂O₃ based devices such as high electron mobility transistors (HEMTs).^{7,8)}

Ga₂O₃ and Al₂O₃ crystalize in different crystal structures, *i.e.*, the β -gallia structure and the corundum structure, respectively. They therefore make solid solutions β -(Al_xGa_{1-x})₂O₃ under certain solubility limit x_{\max} . Hill *et al.* investigated the equilibrium phase diagram of Al₂O₃-Ga₂O₃ system by using powder synthesis technique and reported the lattice parameters of β -(Al_xGa_{1-x})₂O₃.⁹⁾ The phase diagram shows that x_{\max} increases with temperature. For example, x_{\max} is more than 0.6 at 800°C or higher, while x_{\max} is about 0.25 at 650°C, which is the growth temperature of molecular beam epitaxy (MBE) in the present work. Recently, Karnert *et al.* investigated the lattice parameters of their β -(Al_xGa_{1-x})₂O₃ ceramics.¹⁰⁾ The lattice parameters exhibited linear dependence on x when x is 0.3 or lower regardless of the sintering temperature.

A prompt and non-destructive composition measurement is essential in materials development. In the case of relaxed β -(Al_xGa_{1-x})₂O₃, the Al composition can be determined immediately through lattice parameters measurement by x-ray diffraction (XRD). However, the Al composition of strained β -(Al_xGa_{1-x})₂O₃ cannot be estimated directly through lattice parameters measurement since the crystal lattice is elastically deformed and the lattice parameters are different from the relaxed values.

There are a few reports on the estimation of Al composition of strained β -(Al_xGa_{1-x})₂O₃. Oshima *et al.* utilized x-ray photoelectron spectroscopy (XPS) to estimate the Al composition of their films coherently grown on (100) β -Ga₂O₃ substrates by MBE.⁷⁾ However, XPS can collect the data only from the outermost surface (typically a few nanometers deep). Therefore, the measurement can be disturbed when the surface composition is different from that of the body layer. Kaun *et al.* utilized transmission electron microscopy and energy dispersive X-ray spectroscopy (TEM-EDS) to estimate the

Al composition of $\beta\text{-(Al}_x\text{Ga}_{1-x})_2\text{O}_3$ coherently grown on (010) $\beta\text{-Ga}_2\text{O}_3$ by MBE.⁸⁾ However, the measurement is destructive and time-consuming.

In an analogous case of $\text{Al}_x\text{Ga}_{1-x}\text{N}$, Al composition of a coherently grown film has been estimated from the out-of-plane lattice spacing with considering the Poisson effect.¹¹⁾ In the present work, we demonstrate a quick and non-destructive estimation of Al composition of coherently grown (010) $\beta\text{-(Al}_x\text{Ga}_{1-x})_2\text{O}_3$ films using a methodology similar to the case of $\text{Al}_x\text{Ga}_{1-x}\text{N}$.

First, we formulate the relation between the Al composition and the strain along [010]. In the following calculations, the $\beta\text{-(Al}_x\text{Ga}_{1-x})_2\text{O}_3$ layer is assumed to be grown coherently. The unit cells is placed in the Cartesian system so that $[100] \parallel \hat{x}_1$ and $[010] \parallel \hat{x}_2$, where \hat{x}_1 and \hat{x}_2 are the Cartesian unit vectors. We used standard matrix notation to express elastic stiffness tensor \mathbf{c} , stress tensor $\boldsymbol{\sigma}$, and strain tensor $\boldsymbol{\varepsilon}$. The notation rule can be found in Ref. 12, for example. When $\beta\text{-(Al}_x\text{Ga}_{1-x})_2\text{O}_3$ is grown on (010) $\beta\text{-Ga}_2\text{O}_3$ coherently, $\beta\text{-(Al}_x\text{Ga}_{1-x})_2\text{O}_3$ is subjected to in-plane biaxial stress. Accordingly, only in-plane stress components have non-zero values. Similarly, the shear strain ε_4 and ε_6 are zero. Therefore, stress-strain relation in a coherently grown (010) $\beta\text{-(Al}_x\text{Ga}_{1-x})_2\text{O}_3$ film is expressed as follows:

$$\begin{bmatrix} \sigma_1 \\ 0 \\ \sigma_3 \\ 0 \\ \sigma_5 \\ 0 \end{bmatrix} = \begin{bmatrix} c_{11} & c_{12} & c_{13} & 0 & c_{15} & 0 \\ c_{12} & c_{22} & c_{23} & 0 & c_{25} & 0 \\ c_{13} & c_{23} & c_{33} & 0 & c_{35} & 0 \\ 0 & 0 & 0 & c_{44} & 0 & c_{46} \\ c_{15} & c_{25} & c_{35} & 0 & c_{55} & 0 \\ 0 & 0 & 0 & c_{46} & 0 & c_{66} \end{bmatrix} \begin{bmatrix} \varepsilon_1 \\ \varepsilon_2 \\ \varepsilon_3 \\ 0 \\ \varepsilon_5 \\ 0 \end{bmatrix} \quad (1)$$

From the second line in eq. (1), we obtain the following relationship:

$$\varepsilon_2 = -\frac{c_{12}\varepsilon_1 + c_{23}\varepsilon_3 + c_{25}\varepsilon_5}{c_{22}} \quad (2)$$

When the crystal lattice of $\beta\text{-(Al}_x\text{Ga}_{1-x})_2\text{O}_3$ deforms elastically so as to fit that of $\beta\text{-Ga}_2\text{O}_3$, strain components in eq. (2) are given as:

$$\varepsilon_1 = \frac{a_c - a_r}{a_r} \quad (3a)$$

$$\varepsilon_3 = \frac{c_c \sin \beta_c}{c_r \sin \beta_r} - 1 \quad (3b)$$

$$\varepsilon_5 = \frac{c_c \cos \beta_c}{c_r \sin \beta_r} - \frac{a_c \cos \beta_r}{a_r \sin \beta_r} \quad (3c)$$

Here, a_c , c_c , β_c are the in-plane lattice parameters of coherently grown β -(Al_xGa_{1-x})₂O₃, which coincide with those of β -Ga₂O₃ ($a_0 = 12.21$ Å, $b_0 = 3.04$ Å, $c_0 = 5.81$ Å, $\beta_0 = 103.87^\circ$).¹⁰⁾ a_r , c_r , β_r are the in-plane lattice parameters of relaxed β -(Al_xGa_{1-x})₂O₃. Kranert *et al.*¹⁰⁾ have reported these values as functions of x :

$$a_r = a_0 - k_a x \text{ [Å]} \quad (4a)$$

$$b_r = b_0 - k_b x \text{ [Å]} \quad (4b)$$

$$c_r = c_0 - k_c x \text{ [Å]} \quad (4c)$$

$$\beta_r = \beta_0 + k_\beta x \text{ [deg.]} \quad (4d)$$

Here, $k_a = 0.42$, $k_b = 0.13$, $k_c = 0.17$, and $k_\beta = 0.31$. On the other hand, ε_2 can also be expressed as follows:

$$\varepsilon_2 = -\frac{b_r - b_c}{b_r} \quad (5)$$

b_c is the length of b -axis of coherently grown β -(Al_xGa_{1-x})₂O₃, which can be experimentally determined through XRD ω - 2θ measurement. We can determine x by equating eqs. (2) and (5), and solving the equation for x with using eqs. (3a)~(3c) and (4a)~(4d). The result is as follows:

$$x \cong \frac{b_0 - b_c}{b_0} \cdot \left[\frac{k_b}{b_0} + \frac{c_{12}}{c_{22}} \cdot \frac{k_a}{a_0} + \frac{c_{23}}{c_{22}} \cdot \frac{k_c}{c_0} + \frac{c_{25}}{c_{22}} \left(\frac{k_c}{c_0} - \frac{k_a}{a_0} \right) \cot \beta_0 \right]^{-1} \quad (6a)$$

Eq. (6a) is also expressed as follows by using on-axis peak separation of the film and the substrate $\Delta\theta$, and substrate peak position θ_0 :

$$x \cong \Delta\theta \cot\theta_0 \cdot \left[\frac{k_b}{b_0} + \frac{c_{12}}{c_{22}} \cdot \frac{k_a}{a_0} + \frac{c_{23}}{c_{22}} \cdot \frac{k_c}{c_0} + \frac{c_{25}}{c_{22}} \left(\frac{k_c}{c_0} - \frac{k_a}{a_0} \right) \cot\beta_0 \right]^{-1} \quad (6b)$$

To the best of our knowledge, no experimental elastic stiffness tensor is reported about β -(Al_xGa_{1-x})₂O₃. We therefore used a result of first-principles calculation for β -Ga₂O₃. In general, elastic stiffness components show only a slight variation by alloying with small molar fraction, and they tend to vary toward the same direction. Therefore, the variation of their ratio is virtually negligible. The use of elastic stiffness of β -Ga₂O₃ is therefore a good approximation since elastic stiffness components appear as their ratio in eq. (2). The calculation was carried out using the projector augmented wave (PAW) method¹³⁾ under local density approximation (LDA) in the Vienna Ab-Initio Simulation Package (VASP).¹⁴⁾ We used a plane-wave basis set with an energy cutoff $E_{\text{cut}} = 500$ eV and a $2 \times 4 \times 8$ k-point grid. Elastic constants were calculated with the strain-stress method based on the set of six universal deformation modes proposed in ref. 15. The following result was employed in the composition estimation.

$$\begin{bmatrix} 237 & 125 & 147 & 0 & -18 & 0 \\ 125 & 354 & 95 & 0 & 11 & 0 \\ 147 & 95 & 357 & 0 & 6 & 0 \\ 0 & 0 & 0 & 54 & 0 & 19 \\ -18 & 11 & 6 & 0 & 67 & 0 \\ 0 & 0 & 0 & 19 & 0 & 95 \end{bmatrix} [\text{GPa}] \quad (7)$$

Finally, eqs. (6a) is written as:

$$x \cong 15.923 - 5.238 \times b_c [\text{\AA}] \quad (8a)$$

When 020 diffraction is used, eq. (6b) is written as:

$$x \cong 0.4727 \times \Delta\theta_{020} \quad (8b)$$

To examine the methodology described above, we compared the Al compositions estimated by this new method and those measured directly by pulsed laser atom probe tomography (APT).^{16,17)} The β -(Al_xGa_{1-x})₂O₃ films were grown on (010) β -Ga₂O₃ single crystal substrates at 650°C by plasma-assisted MBE. Two different samples were prepared with beam flux ratio $\phi_{\text{Al}} / (\phi_{\text{Al}} + \phi_{\text{Ga}}) = 0.061$ and 0.104. The detail of the growth is described

elsewhere.^{8,18)} High-resolution x-ray diffraction measurements were performed in a triple axis configuration using $\text{CuK}\alpha$ radiation ($\lambda = 1.5406 \text{ \AA}$) at room temperature. Out-of-plane lattice spacing of each film was directly determined through symmetrical ω - 2θ measurement using 020 diffraction. Asymmetrical reciprocal lattice mapping (RSM) using 420 diffraction was carried out to confirm the coherent growth. After the XRD measurements, a 200-nm-thick $\beta\text{-Ga}_2\text{O}_3$ capping layer was additionally grown by MBE on each $\beta\text{-(Al}_x\text{Ga}_{1-x})_2\text{O}_3$ layer before producing a tip sample for APT to ensure that the whole thickness of the $\beta\text{-(Al}_x\text{Ga}_{1-x})_2\text{O}_3$ layer was included in the tip. APT samples were prepared by focus ion beam (FIB) technique. About 150 nm wide needle like tips were polished using a FEI Helios Dual Beam Nanolab 650 instrument, milled at 30 kV and followed by a final cleaning at 5 kV. The experiment was carried out using a Cameca LEAP 3000X atom probe instrument equipped with a 532 nm green pulsed laser. The laser energy is around 0.2 nJ, the tip temperature was about 40K and evaporation rate was 1%.

Figures 1(a) and (b) show the XRD ω - 2θ profiles of the $\beta\text{-(Al}_x\text{Ga}_{1-x})_2\text{O}_3$ films. Each profile exhibited a single $\beta\text{-(Al}_x\text{Ga}_{1-x})_2\text{O}_3$ 020 diffraction peak with thickness fringes. The out-of-plane lattice spacing of the films were determined to be (a) 3.019 \AA and (b) 3.009 \AA , respectively. The thicknesses of the two films determined from the fringe spacing were 130 and 127 nm, respectively.

Figure 2(a) and (b) show the RSMs of the two films. The 420 peaks of $\beta\text{-Ga}_2\text{O}_3$ and $\beta\text{-(Al}_x\text{Ga}_{1-x})_2\text{O}_3$ appeared at the same q_x position in each RSM, indicating that the $\beta\text{-(Al}_x\text{Ga}_{1-x})_2\text{O}_3$ films were grown coherently.

Figure 3(a) and (b) show the depth profiles of the Al and Ga compositions for the two films measured by APT. The film composition was nearly uniform along the growth direction of the $\beta\text{-(Al}_x\text{Ga}_{1-x})_2\text{O}_3$ films. The average Al composition in each film was 0.120 and 0.168. These values are significantly higher than those expected from the beam flux ratio. This is probably due to the low incorporation efficiency of Ga because of the formation of volatile suboxide Ga_2O .^{12,19)}

The calculated Al composition of coherently grown $\beta\text{-(Al}_x\text{Ga}_{1-x})_2\text{O}_3$ is shown in Fig. 4 as a function of b_c together with the averaged APT results. We also show the relationship for relaxed $\beta\text{-(Al}_x\text{Ga}_{1-x})_2\text{O}_3$ reported by Kranert *et al.*¹⁰⁾ for comparison. The calculated result for coherent films is in good agreement with the APT results, while the application of the relaxed line to the fully strained films results in significant overestimation.

In summary, the Al composition of $\beta\text{-(Al}_x\text{Ga}_{1-x})_2\text{O}_3$ films coherently grown on (010)

β -Ga₂O₃ by MBE was successfully estimated by conventional XRD ω - 2θ measurement with considering the Poisson effect in the monoclinic system. Coherent growth was confirmed by RSM measurement. The elastic stiffness tensor of β -Ga₂O₃ obtained by first-principle calculation was utilized in the estimation. The result was in a close agreement with the Al compositions directly measured by APT. This methodology enables us to estimate the Al composition of coherently grown β -(Al_xGa_{1-x})₂O₃ in a rapid and non-destructive manner, and thus it will boost the development of high-performance β -Ga₂O₃ based devices.

Acknowledgments

This work was supported by the Air Force Office of Scientific Research (AFOSR, Program Manager Dr. Ali Sayir) through grant # FA9550-14-1-0112. Additional support for J.S.S. was provided by the MRSEC Program of the U.S. National Science Foundation under Award No. DMR-1121053.

References

- 1) H. H. Tappin: Phys. Rev. **140**, A316 (1965).
- 2) M. R. Lorenz, J. F. Woods, and R. J. Gambino: J. Phys. Chem. Solids **28**, 403 (1967).
- 3) M. Orita, H. Ohta, M. Hirano, and H. Hosono: Appl. Phys. Lett. **77**, 4166 (2000).
- 4) K. Sasaki, A. Kuramata, T. Masui, E.G. Villora, K. Shimamura, and S. Yamakoshi, Appl. Phys. Express **5**, 035502 (2012).
- 5) M. Higashiwaki, K. Sasaki, A. Kuramata, T. Masui, S. Yamakoshi, Appl. Phys. Lett. **100**, 013504 (2012).
- 6) M. Higashiwaki, K. Sasaki, T. Kamimura, M.H. Wong, D. Krishnamurthy, A. Kuramata, T. Masui, S. Yamakoshi, Appl. Phys. Lett. **103**, 123511 (2013).
- 7) T. Oshima, T. Okuno, N. Arai, Y. Kobayashi, and S. Fujita, Jpn. J. Appl. Phys. **48**, 070202 (2009).
- 8) S. W. Kaun, F. Wu, James S. Speck, J. Vac. Sci. Technol. A **33**, 041508 (2015).
- 9) V. G. Hill, R. Roy, and E. F. Osborn, J. Am. Ceram. Soc. **35**, 135 (1952).
- 10) C. Kranert, M. Jenderka, J. Lenzner, M. Lorenz, H. von Wenckstern, R. Schmidt-Grund, and M. Grundmann, J. Appl. Phys. **117**, 125703 (2015).
- 11) T. Takeuchi, H. Takeuchi, S. Sota, H. Sakai, H. Amano, and I. Akasaki, Jpn. J. Appl. Phys. **36**, L177 (1997).
- 12) J. F. Nye, "Physical Properties of Crystals: Their Representation by Tensors and Matrices", Oxford Univ. Press (1985).

- 13) P. Blöchl, Phys. Rev. B **50**, 17953 (1994).
- 14) J. Hafner, J. Comput. Chem. **29**, 2044 (2008).
- 15) R. Yu, J. Zhu, H.Q. Ye, Comput. Phys. Comm. **181**, 671 (2010).
- 16) T. F. Kelly & M. K. Miller, The Review of Scientific Instruments, **78**, 031101 (2007).
- 17) B. Gault, M. P. Moody, J. M. Cairney, S. P. Ringer, “Atom Probe Microscopy” (Springer Science & Business Media, 2012).
- 18) H. Okumura, M. Kita, K. Sasaki, A. Kuramata, M. Higashiwaki, and J. S. Speck, Applied Physics Express **7**, 095501 (2014).
- 19) P. Vogt and O. Bierwagen, Appl. Phys. Lett. **108**, 072101 (2016).

Figure Captions

Fig. 1. XRD ω - 2θ scan profiles of β -(Al_xGa_{1-x})₂O₃ films. (a) $\phi_{\text{Al}} / (\phi_{\text{Al}} + \phi_{\text{Ga}}) = 0.061$, (b) $\phi_{\text{Al}} / (\phi_{\text{Al}} + \phi_{\text{Ga}}) = 0.104$.

Fig. 2. RSMs of β -(Al_xGa_{1-x})₂O₃ films. (a) $\phi_{\text{Al}} / (\phi_{\text{Al}} + \phi_{\text{Ga}}) = 0.061$, (b) $\phi_{\text{Al}} / (\phi_{\text{Al}} + \phi_{\text{Ga}}) = 0.104$.

Fig. 3. Depth profiles of Al and Ga compositions of β -(Al_xGa_{1-x})₂O₃ films measured by APT. (a) $\phi_{\text{Al}} / (\phi_{\text{Al}} + \phi_{\text{Ga}}) = 0.061$, (b) $\phi_{\text{Al}} / (\phi_{\text{Al}} + \phi_{\text{Ga}}) = 0.104$.

Fig. 4. Relationships between b_c and Al composition x . Error bars show $\pm 2\sigma$. The calculated result for coherent films is approximated by eq. (8a).

Figures

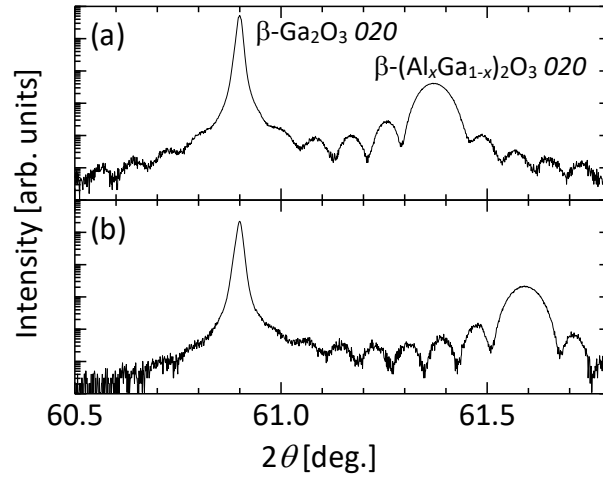


Fig. 1.

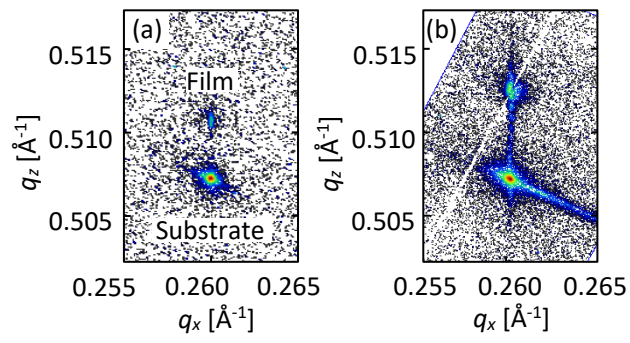


Fig. 2.

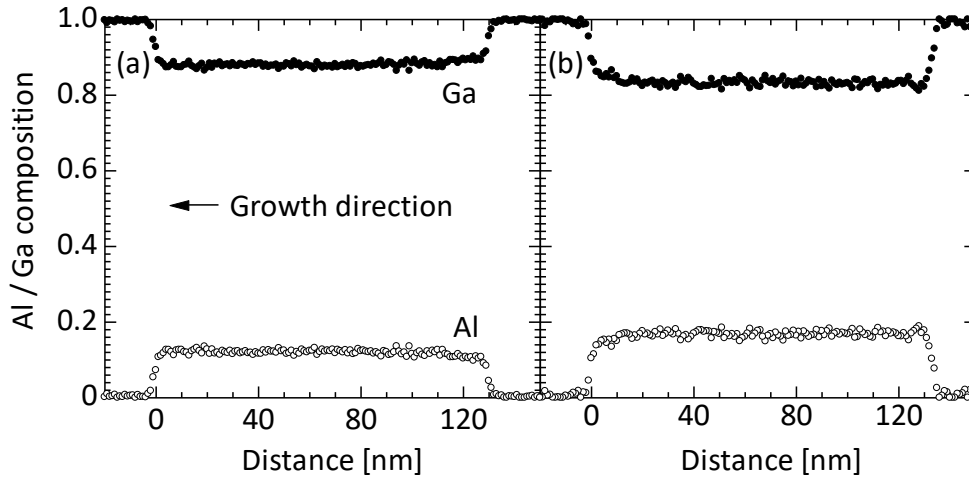


Fig. 3.

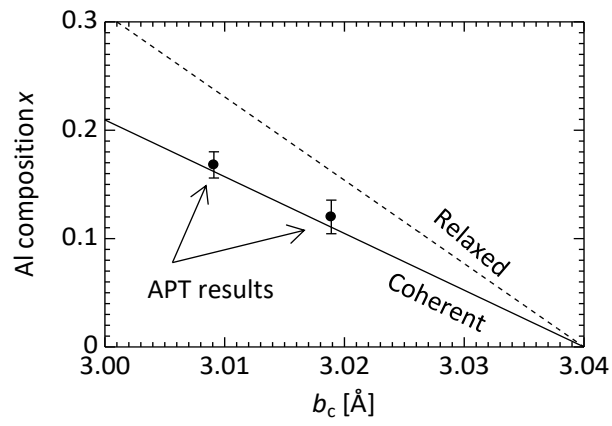


Fig. 4.